A subpopulation of monocytes in normal human blood has significant magnetic susceptibility; quantification and potential implications

J. Kim[1,a], **J. Gomez-Pastora**[1,a], **M. Weigand**[1], **Potgieter Marnie**[2], **N. Walters**[1], **E. Reategui**[1], **A. Palmer**[1], **M. Yazer**[3], **M. Zborowski**[4], **J.J. Chalmers**[1,†]

[1]William G. Lowrie Department of Chemical and Biomolecular Engineering, The Ohio State University,320 Koffolt Laboratories, 151 West Woodruff Avenue, Columbus, OH 43210

[2]Centre for Microbial Ecology and Genomics, University of Pretoria, Pretoria, South Africa, 0002

[3]Department of Pathology, University of Pittsburgh and The Institute for Transfusion Medicine, University of Pittsburgh, 3636 Blvd of the Allies, Pittsburgh, PA 15213

[4]Department of Biomedical Engineering, Cleveland Clinic, 9500 Euclid Avenue, Cleveland, OH 44195.

Abstract

The presence of iron in circulating monocytes is well known as they play essential roles in iron recycling. Also, the storage of this metal as well as its incorrect uptake and/or release are important data to diagnose different pathologies. It has been demonstrated that iron storages in human blood cells can be measured through their magnetic behavior with high accuracy, however, the magnetic characteristics of monocytes have not been reported so far to the best of our knowledge. Therefore, in this work, we report, for the first time, the physical and magnetic properties of human monocytes, along with plasma platelets, oxyhemoglobin red blood cells (oxyHb-RBCs) and methemoglobin red blood cells (metHb-RBCs). The different cell populations were separated by Ficoll-density gradient centrifugation, followed by a flow sorting step to isolate monocytes from peripheral blood mononuclear cells. The different fractions were analyzed by Coulter Counter (for determining the size distribution and concentration) and the sorted monocytes were qualitatively analyzed on ImageStream, a state-of-the-art imaging cytometer. The analysis of the Coulter Counter and ImageStream data suggests that although there exists contamination in the monocyte fraction, the integrity of the sorted monocytes appears to be intact and the concentration was high enough to precisely measure their magnetic velocity by Cell Tracking Velocimetry (CTV). Surprisingly, monocytes reported the highest magnetic mobility from the four fractions under analysis, with an average magnetic velocity 7.8 times higher than MetHb-RBCs, which is the only type of cells with positive magnetic velocities. This value is equivalent to a susceptibility

[†] To whom correspondence should be addressed: Jeffrey J. Chalmers, William G. Lowrie Department of Chemical and Biomolecular Engineering, The Ohio State University, 151 West Woodruff Avenue, Columbus, OH 43210, Chalmers.1@osu.edu, Tel: (614)292-2727.
[a]James Kim and Jenifer Gomez-Pastora contributed equally to this work.

2.5 times higher than the value reported by fresh MetHb-RBCs. It should be noted that this is the first study that reports that a subpopulation of human monocytes is much more magnetic than MetHb-RBCs, opening the door to the possible isolation of human monocytes by label-free magnetic techniques. Also, this paper reports the risk of using negative magnetic isolation techniques for monocytes, which have been suggested by different researchers, and that will result in the loss of the magnetic subpopulation of monocytes.

Keywords

monocytes; platelets; RBCs; magnetic susceptibility; cell tracking velocimetry; imaging cytometer

1.   Introduction

Monocytes are circulating blood cells and account for 2–8% of leukocytes. They spend only a short time in the circulation (approximately 24 hours) before entering the tissue where they become macrophages (1,2). Monocytes play important roles in the inflammatory response; they are also able to phagocytose pathogens and damaged cells (2,3). Therefore, isolation of monocytes from complex media such as blood is has a range of applications including the potential to provide insight into various normal and abnormal cell recycling.

Whereas there exist positive and negative magnetic separation techniques for monocyte isolation (4,5), very little information is available regarding the intrinsic magnetic properties of these cells. However, multiple studies have demonstrated the presence of iron within monocytes (6) and this fact may imply that they are not as diamagnetic as most cells and has typically been assumed. In fact, monocytes are involved in the recycling of iron, and hence, they play central roles in iron homeostasis. It has been suggested that the retention of iron within monocytes and macrophages results in a reduced availability of the metal for invading pathogens which need iron for their growth and proliferation. Moreover, iron within monocytes and macrophages catalyzes the formation of toxic hydroxyl radicals, which is an important part of the immune defense armory against invading pathogens (7).

Monocytes/macrophages have evoked different pathways by which they can acquire iron, including transferrin mediated iron uptake, transmembrane uptake of ferrous and possibly also of ferric iron, iron acquisition via lactoferrin receptors, ferritin receptors or via erythrophagocytosis (8,9). Also, extracellular- and intracellular-free hemoglobin (Hb) (a strong oxidant catalyst that could lead to cell damage in the arterial wall) is cleared by CD163, a scavenger receptor present on the surface of circulating monocytes and tissue macrophages (10,11). In addition, monocytes express CD91, the hemopexin receptor, which takes up heme captured by the heme binding protein, hemopexin, resulting in induction of heme oxygenase and iron accumulation in monocytes (12). Among all of these iron acquisition mechanisms, the most important one is iron uptake via erythrophagocytosis (7,13). After a mean half-life of 120 days, senescent erythrocytes express increased quantities phosphatidylserine residues on their surfaces which are then recognized by macrophage/monocyte surface receptors leading to attachment of erythrocytes and subsequent phagocytosis (14). It has been reported that macrophages can phagocytose up to

three times more erythrocytes than do monocytes (7,15). Recent studies have shown that in humans, erythrocyte damage resulted in erythrocyte accumulation in circulating classical monocytes along with higher intracellular and serum iron levels (16).

Importantly, monocytes release iron, which is essential for iron re-circulation from degraded erythrocytes. Since ferroportin is the only known iron exporter, the expression of ferroportin in monocytes and macrophages is positively associated with erythrophagocytosis. Reduced ferroportin mRNA and protein expression results in a diminished iron release from cytokine-stimulated monocytes, which points to the gatekeeper function of ferroportin in controlling iron export/iron retention in monocytes (17). Recent evidence suggests that monocytes and macrophages are able to release heme which may be traced back to the expression of a heme export protein (7).

Iron uptake and release by monocytes are regulated at multiple steps, which are differently affected by pro- and anti-inflammatory cytokines. These regulation mechanisms can be affected by different diseases. One study (18) has investigated the release of erythrocyte-derived iron from purified human monocytes obtained from healthy volunteers and hereditary hemochromatosis (HH) patients. It was found that the iron was released from the monocytes in the form of ferritin, Hb, and as non-protein bound low molecular weight iron (LMW-Fe). A high percentage of the total amount of iron was released as Hb both by viable normal and HH monocytes, suggesting that iron release as Hb is a physiologic process, which may occur whenever the erythrocyte-processing capacity of macrophages is exceeded. Most remarkably, HH monocytes released twice as much iron in a LMW form as control cells. Iron released in the form of LMW-Fe readily binds to plasma transferrin and may contribute to the high transferrin saturation and the occurrence of circulating non-transferrin-bound iron observed in HH patients. Other studies have shown that monocyte-derived macrophages from HH patients accumulate less iron from transferrin than macrophages from normal individuals (19). Analogously, iron bound to apoferritin instead of transferrin in monocytes has been suggested as a contributory factor in the pathogenesis of anemia of chronic disease (ACD) (20). In this case, the failure of iron utilization is due to its impaired release from the monocyte-macrophage system to circulating transferrin, making the iron unavailable for erythropoiesis. Also, hepcidin, a master regulator of iron homeostasis, is produced in small amounts by inflammatory monocytes/macrophages. Chronic immune activation leads to iron retention within monocytes/macrophages and the development of ACD (21). High iron stores within monocytes have also been linked to an increased risk of atherosclerosis, as it affects the interaction of monocytes to endothelium, an initial event in the formation of atherosclerotic plaques. Non–transferrin-bound iron increases the level of intracellular labile iron, which promotes monocyte recruitment to endothelium and may thereby contribute to the pathogenesis of atherosclerosis (22,23). Therefore, iron storage within monocytes or its incorrect uptake and/or release are important data to further evaluate different diseases.

One possibility method to analyze the iron content inside a cell, and in this case a monocyte, is the measurement of the cell's magnetic susceptibility. Over the years, we have been developing a way to quantitatively characterize the magnetic behavior of biological entities with an instrument referred to as Cell Tracking Velocimetry (CTV) (24–27). This CTV

instrument characterizes both the magnetically induced velocity, u_m and gravity induced settling velocity, u_s, using a combination of computer tracking algorithms of microscopic images captured with a charged couple device, CCD, camera. The camera captures the movement of the samples in the region of interest, ROI; within this ROI, a high, and well characterized, magnetic energy gradient in the horizontal direction is created and a nearly zero magnetic energy gradient in the vertical direction. When a cell is placed in this ROI, experimentally measured horizontal and vertical velocities are measured which can be related to specific cellular and field properties by:

$$u_m = \frac{(\chi_{Cell} - \chi_{Fluid})V_{Cell}}{3\pi D_{Cell}\eta}S_m \tag{1}$$

$$u_s = \frac{(\rho_{Cell} - \rho_{Fluid})V_{Cell}}{3\pi D_{Cell}\eta}g \tag{2}$$

where χ_{cell} and χ_f is the magnetic susceptibility of cell and the buffer, ρcell, ρf are density of the cell/fluid, D_{cell} and V_{cell} is the diameter and volume of cell, η and is the viscosity of the suspending fluid and g gravity (9.8 m/s^2), and S_m defined as

$$S_m = \frac{\left|\nabla B^2\right|}{2\mu_0} \tag{3}$$

where μ_0 and B are the permeability of free space and flux density of the source.

With an analogy to electrophoretic induced motion, we have previously introduced a further term, referred to as magnetophoretic mobility, m:

$$m = \frac{u_m}{S_m} = \frac{(\chi_{cell} - \chi_f)V_{cell}}{3\pi D_{cell}\eta} \tag{4}$$

As with electrophoretic motion, the magnetophoretic mobility allows straight forward comparisons and applications to other systems/devices in which the value of S_m is known (28).

In this study, we describe for the first time the magnetic behavior of human monocytes, by observing their magnetic velocity through CTV, along with plasma platelets, oxyhemoglobin red blood cells (oxyHb-RBCs) and methemoglobin red blood cells (metHb-RBCs) as a reference/comparative data. We will also observe their physical characteristics through state-of-the-art imaging cytometer to correlate their magnetic and physical properties.

2. Materials and Methods

2.1. Sample Preparation

Human whole blood from five healthy subjects (two females and three males) was collected with informed consents according to a protocol approved by the Institutional Review Board (IRB) from The Ohio State University (protocol number 38334). Approximately 15 ml of blood was drawn and collected into 10 mL tubes containing EDTA anticoagulant. Then, using Ficoll – Paque PREMIUM density gradient media (GE Healthcare, Sweden), 12 mL of the drawn-out blood was separated into four populations following the manufacturer's instructions: i) RBCs (accumulated at the bottom of the centrifugation tube); ii) Ficoll media, that was later discarded; iii) peripheral blood mononuclear cells (PBMCs), which can be distinguished as a grayish colored ring over the Ficoll media and contain the monocytes; and iv) plasma layer containing platelets. The separated populations were collected in independent tubes with appropriate buffers as described below. Also, their concentration and size distribution were characterized using B23005 Multisizer 4e Coulter Counter before further processing. In Figure 1, the workflow of the sample preparation procedure is schematized.

RBCs.—RBCs were divided into two aliquots designated "metHb containing RBCs" and "oxygenated RBCs". The RBCs were collected from the bottom of the centrifugation tube and washed with PBS and were left in the room oxygen for 10 minutes to ensure they were in the oxyHb state. The MetHb-RBCs were obtained after treating the washed-RBCs with $NaNO_2$ as previously reported in the literature (24,27,29).

Monocytes.—PBMCs were collected after performing the density gradient centrifugation and further purified by two additional washing steps following the instructions of the manufacturer. Next, the PBMCs were washed with PBS and incubated in 1 mL of FACS staining buffer (Invitrogen, US) for approximately 1 hour at room temperature in the dark with the following fluorochrome-conjugated antibodies (BD Biosciences, US): Alexa Fluor® 488 Mouse Anti-Human CD14 (targeting monocytes) and APC Mouse Anti-Human CD61 (in order to evaluate the possible contamination of platelets).

Platelets.—Platelets were processed as collected from the top plasma layer after centrifugation with the Ficoll – Paque PREMIUM density gradient media. As will be presented below, insufficient platelets were obtained for subsequent analysis since Ficoll-Paque is optimize for nucleated cell recovery. Consequently, platelets were enriched with RegenKit BCT centrifuge tubes (RegenLab USA) specifically optimized for platelet purification and enrichment. This procedure was performed for only one of the donor samples and the results are presented in the supplemental information.

2.2. Flow Cytometry

PBMCs incubated with Alexa Fluor® 488 Mouse Anti-Human CD14 were loaded onto flow cytometer BD FACS ARIA III (BD Biosciences, US) and the CD14+ population was collected as shown in Figure 1. The sort was operated until approximately 200,000 events

were collected. An aliquot designated for Imagestream-analysis was also prepared after sorting.

2.3. Imagestream

CD14+ monocytes and CD14+CD61+ entities dyed with both Alexa Fluor® 488 and APC were loaded onto the imaging cytometer Amnis ImageStreamX Mark II and 488/633 positive samples' images were recorded.

2.4. Cell Tracking Velocimetry

The CTV instrument configuration reported in this study has been reported in our previous publications (24). The following procedure was used to characterize u_m and u_s. The samples were loaded into the CTV channel, (each fraction had approximately the same volume of 1 ml) and the channels were sealed on both ends using Hamiltonian valves, and approximately 20 s were taken to wait for the fluid environment in the channel to reach steady state. After the samples began to settle, images of the samples' movement were captured (50 video images, 1 s interval) and further processed using in-house analysis program for calculation of the magnetic/settling velocity.

3. Results and discussion

3.1. Coulter Counter characterization of the fractions obtained by Ficoll density gradient separation

The Ficoll density gradient separated entities were ran through Coulter-Counter for size-distribution characterization, which is shown in Table 1 and Figure 2. The size distribution of Ficoll-separated RBCs and plasma platelets match with the literature data (RBCs: 4–6 μm, platelets 2–3 μm), except for the PBMCs. However, the PBMCs fraction appears to have three subpopulations as shown in Figure 2, and they appear to match the reported diameter values of platelets, lymphocytes (7 μm) and monocytes (8.79 μm) (30).

3.2. Monocyte isolation by FACS

To further enrich for the monocyte population, we included a FACS step to isolate the monocytes from platelets and lymphocytes. Since monocytes are frequently associated with platelets, we incubated the PBMCs fraction with two different fluorescently labeled antibodies, prior to FACS, for separating those cells expressing CD14 (monocytes) and CD61 (platelets). The results are presented in Figure 3 for the blood obtained from one of our donors, which is representative of all of the donors. The sorted monocyte population is represented by a high fluorescence intensity of Alexa Fluor 488 (P4, labeled as FITC in Figure 3). We observed a population of platelets bound to monocytes (P6), which are characterized by the high intensity fluorescence in both the FITC and APC channel. P5 is the negative fraction, comprising the negative CD14 and CD61 cells, which was later discarded. The presence of a population of pure platelets was not observed, which may indicate that all the platelets obtained within the PBMCs get rapidly attached to the surface of monocytes. Nonetheless, this population is low in number in comparison to P4, and it was not further analyzed since it was not possible to precisely measure the magnetic velocity of these complexes due to their low concentration.

The sorted P4 fraction, comprising a pure population of monocytes was later analyzed on Coulter Counter; presumed monocytes can be easily distinguished as the largest cells in this specific blood fraction. The results are presented in Figure 4. In addition to the CD14+ cells, a large proportion of what is presumed to be cell debris was consistently observed for the samples obtained from all the donors. We attribute this contamination to the possible cell destruction during FACS operation (31). It has been reported that dead cells bind non-specifically to antibodies (32), which could be the major source of the contamination that we observed within the monocyte population. Nevertheless, the concentration of cells larger than 6 μm is relatively high, which is attributed to the sorted monocytes that were not destroyed by FACS.

3.3. Analysis of the isolated monocytes by ImageStream

The sorted monocytes were qualitatively analyzed on ImageStream. The equipment was loaded with a small aliquot of the CD14+ fraction and the CD14+CD61+ fraction and the samples were run until at least 500 pictures were taken from individual cells/complexes. The images reported for both fractions were very similar, as monocytes were attached to other cells as presented in Figure 5 for the P4 fraction. It can be seen that monocytes are bound to different type of cells, smaller in size, that were not fluorescent in comparison to the stained monocytes (seen in green in the FITC channel). The cellular integrity for these monocytes appears to be intact after sorting, and therefore, they were analyzed on the CTV along with the platelets and RBCs to evaluate their magnetic velocity.

3.4. Magnetic mobility of fresh blood fractions – CTV results

To measure the magnetic/settling velocities of the four fractions our CTV apparatus was used. In Figure 6, we present representative trajectories; platelets (Figure 6 a), OxyHb-RBCs (Figure 6 b), MetHb-RBCs (Figure 6 c) and monocytes (Figure 6 d) inside the CTV for 50 s and for one of the donors. The vertical trajectories for the platelets and OxyHb-RBCs are consistent with our previous publications, and indicate very low magnetic mobility (i.e. diamagnetic). In contrast, MetHb-RBCs are slightly deflected in diagonal inside the ROI, i.e. they are deflected towards the right direction, which is consistent with a positive magnetic force acting on them due to their paramagnetic behavior in PBS as we have previously reported (24). However, the CTV analysis of monocytes implied the presence of two population among monocytes, a very strong magnetic population and non-magnetic population as shown in Figure 6d. In fact, the trajectories followed by this magnetic subfraction displays a very high magnetic velocity as they move almost horizontally from left to right within the ROI.

Histogram comparisons between the magnetic and settling velocities for the four fractions is presented in Figure 7 for the same donor sample shown in Figure 6. It can be seen that whereas platelets and OxyHb-RBCs are concentrated in the zone where the magnetic velocity is close to 0, there is a variability in their settling velocity, especially for platelets, which could be attribute to their different size/density. On the other hand, MetHb-RBCs are slightly displaced to the right, with magnetic velocities close to 0.001 mm/s (and reporting a similar value for the settling velocity). Two populations of monocytes are easily distinguished in the figure. The non-magnetic monocytes are concentrated at $u_m \approx 0$ and u_s

≈ 0.0015 mm/s, whereas the magnetic population shows u_m values as high as 0.27 mm/s. It should be noted that for all the fractions, the reported settling velocity is around 0.001 mm/s. However, the magnetic velocity shows more variability for the different fractions and was next analyzed for all the donors.

The inclusive analysis of the magnetic velocity for all the fractions and all the donor samples is presented in Figure 8. We obtained consistent magnetic velocities for both types of RBCs for all the donor samples, but the variability for platelets and monocytes is high and varies depending on the donor sample. (Table 2) However, not all the samples contain "magnetic" platelets, whereas a positive magnetic velocity for monocytes was observed for all the donors, as seen in Figure 8. For example, the magnetic velocity of the platelets from donor 2 is close to zero, and generally, the more magnetic the monocytes are, the higher magnetic velocity is observed for platelets. Based on this correlation, we believe that the platelets collected from the plasma layer and analyzed on CTV could have been contaminated with monocytes, as both layers are in contact after the Ficoll density gradient separation was performed and it is difficult to isolate both type of cells with high selectivity. Furthermore, the size analysis performed on plasma samples corroborates this contamination as there exist cell entities with sizes larger than 6 μm in plasma, which could be inferred from Figure 2, and this contamination was observed for all the donor samples to a greater or lesser extent. Therefore, the platelet population from one of the donors was fractionated/characterized using RegenKit BCT centrifuge tubes, and the result returned magnetic velocity of the platelet fraction to be close to zero (Shown in Supplemental Information). Also, there seems to be two sub-group of monocytes based on their magnetic velocity, so each population's average magnetic velocity was calculated separately, which is presented in Figure 8b and Table 3.

4. Conclusion

In this study, we have reported, for the first time, the magnetic analysis of human fresh blood cells with an emphasis on monocytes. Monocytes are known to contain iron as they take part in iron recycling along with tissue macrophages, and the measurement of this metal within monocytes, including its uptake and release from the cell, could be useful to diagnose different pathologies. Although we have demonstrated before that iron storage in human blood cells can be measured through their magnetic behavior with high accuracy (24), the magnetic characteristics of monocytes have not been reported so far, to the best of our knowledge. Therefore, in this work, we have isolated monocytes from human fresh whole blood and characterized their physical and magnetic properties, along with plasma platelets, oxyHb-RBCs and metHb-RBCs as a reference/comparative data.

The different cell populations were separated by Ficoll-density gradient centrifugation, followed by a FACS step to isolate monocytes from PBMCs. The different fractions were later analyzed by Coulter Counter and CTV, and the sorted monocytes were qualitatively analyzed on ImageStream, imaging cytometer. The analysis of the Coulter Counter and ImageStream data suggests that the sorted monocytes are attached to other cells, different in size. Nonetheless, the integrity of the sorted monocytes appears to be intact and the concentration reported was high enough to precisely measure their magnetic mobility on the

CTV system. The magnetic velocity and settling velocity for the four fractions was measured by tracking the cell trajectories inside the CTV apparatus. Whereas all the cell types reported similar settling velocities, the magnetic velocities varied depending on the cell population analyzed. For instance, oxyHb-RBCs behave as non-magnetic (i.e. diamagnetic) but MetHb-RBCs display a paramagnetic behavior in PBS. Surprisingly, monocytes reported the highest magnetic mobility from the four fractions under analysis, with an average magnetic velocity 7.8 times higher than MetHb-RBCs. Finally, positive magnetic velocities were also observed for some of the plasma samples, which could either mean that platelets may contain iron or that monocyte contamination was present in these samples as we believe.

It should be noted that this is the first study that reports that a subpopulation of human monocytes is much more magnetic than MetHb-RBCs, opening the door to the possible isolation of human monocytes by label-free magnetic techniques. Also, this paper reports the risk of using negative magnetic isolation techniques for monocytes, which have been suggested by different researchers (4,33,34). In fact, the use of these isolation techniques will result in the loss of monocytes and thus, the resultant isolated sample will not be complete. However, there are different issues that were not covered in this work and that need to be further addressed, such as the cross contamination of platelets and monocytes in the individual samples, along with the characteristics of the magnetic monocytes versus the non-magnetic monocytes, which are the focus of our future work.

Supplementary Material

Refer to Web version on PubMed Central for supplementary material.

ACKNOWLEDGEMENTS

REFERENCES

1. Monie TP. The innate immune system: a compositional and functional perspective. London: Academic Press; 2017 19 p.

2. Ashton N Physiology of red and white blood cells. Anaesth. Intensive Care Med. 2007;8:203–208.

3. Auffray C, Sieweke MH, Geissmann F. Blood monocytes: development, heterogeneity, and relationship with dendritic cells. Annu. Rev. Immunol. 2009;27:669–692. [PubMed: 19132917]

4. Bhattacharjee J, Das B, Mishra A, Sahay P, Upadhyay P. Monocytes isolated by positive and negative magnetic sorting techniques show different molecular characteristics and immunophenotypic behavior. F1000Res. 2017;6:2045. [PubMed: 29636897]

5. Weiss R, Gerdes W, Leonhardt F, Berthold R, Sack U, Grahnert A. A comparative study of two separation methods to isolate monocytes. Cytometry, Part A 2018; DOI: 10.1002/cyto.a.23633.

6. Prus E, Fibach E. Flow cytometry measurement of the labile iron pool in human hematopoietic cells. Cytometry, Part A 2008;73A:22–27.

7. Weiss G Iron metabolism in the anemia of chronic disease. Biochim. Biophys. Acta 2009;1790:682–693. [PubMed: 18786614]

8. Iron Weiss G. and immunity: a double-edged sword. Eur. J. Clin. Invest. 2002;32:70–78. [PubMed: 11886435]

9. Birgens HS, Kristensen LØ, Borregaard N, Karle H, Hansen NE. Lactoferrin-mediated transfer of iron to intracellular ferritin in human monocytes. Eur. J. Haematol. 1988;41:52–57. [PubMed: 3402586]

10. Hvidberg V, Maniecki MB, Jacobsen C, Højrup P, Møller HJ, Moestrup SK. Identification of the receptor scavenging hemopexin-heme complexes. Blood 2005;106:2572–2579. [PubMed: 15947085]

11. Rubio-Navarro A, Villalobos JMA, Lindholt JS, Buendía I, Egido J, Blanco-Colio LM, Samaniego R, Meilhac O, Michel JB, Martín-Ventura JL, Moreno JA. Hemoglobin induces monocyte recruitment and CD163-macrophage polarization in abdominal aortic aneurysm. Int. J. Cardiol 2015;201:66–78. [PubMed: 26296046]

12. Anderson GJ, McLaren GD. Iron Physiology and Pathophysiology in Humans. New York: Springer; 2012 214 p.

13. Knutson M, Wessling-Resnick M. Iron metabolism in the reticuloendothelial system. Crit. Rev. Biochem. Mol. Biol. 2003;38:61–88. [PubMed: 12641343]

14. de Back DZ, Kostova EB, van Kraaij M, van den Berg TK, van Bruggen R. Of macrophages and red blood cells; A complex love story. Front. Physiol. 2014;5:9. [PubMed: 24523696]

15. Raha-Chowdhury R, Williams BJ, Worwood M. Red cell destruction by human monocytes - changes in intracellular ferritin concentration and phenotype. Eur. J. Haematol. 1993;50:26–31. [PubMed: 8436211]

16. Theurl I, Hilgendorf I, Nairz M, Tymoszuk P, Haschka D, Asshoff M, He S, Gerhardt LMS, Holderried TAW, Seifert M, Sopper S, Am Fenn, Anzai A, Rattik S, McAlpine C, Theur M, Wieghofer P, Iwamoto Y, Weber GF, Harder NK, Chousterman BG, Arvedson TL, McKee M, Wang F, Lutz OMD, Rezoagli E, Babitt JL, Berra L, Prinz M, Nahrendorf M, Weiss G, Weissleder R, Lin HY, Swirski FK. On-demand erythrocyte disposal and iron recycling requires transient macrophages in the liver. Nat. Med. 2016;22:945–951. [PubMed: 27428900]

17. Ludwiczek S, Aigner E, Theurl I, Weiss G. Cytokine-mediated regulation of iron transport in human monocytic cells. Blood 2003;101:4148–4154. [PubMed: 12522003]

18. Moura E, Noordermeer MA, Verhoeven N, Verheul AFM, Marx JJM. Iron release from human monocytes after erythrophagocytosis in vitro: an investigation in normal subjects and hereditary hemochromatosis patients. Blood 1998;92:2511–2519. [PubMed: 9746792]

19. Kong W, Duan X, Shi Z, Chang Y. Iron metabolism in the mononuclear phagocyte system. Prog. Nat. Sci. 2008;18:1197–1202.

20. Smith MA, Knight SM, Maddison PJ, Smith JG. Anemia of chronic disease in rheumatoid arthritis: effect of the blunted response to erythropoietin and of interleukin 1 production by marrow macrophages. Ann. Rheum. Dis. 1992;51:753–757. [PubMed: 1616358]

21. Theurl I, Theurl M, Seifert M, Mair S, Nairz M, Rumpold H, Zoller H, Bellmann-Weiler R, Niederegger H, Talasz H, Weiss G. Autocrine formation of hepcidin induces iron retention in human monocytes. Blood 2008;111:2392–2399. [PubMed: 18073346]

22. Kartikasari AER, Georgiou NA, Visseren FLJ, van Kats-Renaud H, van Asbeck BS, Marx JJM. Intracellular labile iron modulates adhesion of human monocytes to human endothelial cells. Arterioscler. Thromb. Vasc. Biol. 2004;24:2257–2262. [PubMed: 15486315]

23. Kartikasari AER, Visseren FLJ, Marx JJM, van Mullekom S, van Kats-Renaud JH, van Asbeck BS, Ulfman LH, Georgiou NA. Intracellular labile iron promotes firm adhesion of human monocytes to endothelium under flow and transendothelial migration. Iron and monocyte–endothelial cell interactions. Atherosclerosis 2009;205:369–375. [PubMed: 19187935]

24. Chalmers JJ, Jin X, Palmer AF, Yazer MH, Moore L, Amaya P, Park K, Pan X, Zborowski M. Femtogram resolution of iron content on a per cell basis: ex vivo storage of human red blood cells leads to loss of hemoglobin. Anal. Chem. 2017;89:3702–3709. [PubMed: 28230974]

25. Moore LR, Milliron S, Williams PS, Chalmers JJ, Margel S, Zborowski M. Control of magnetophoretic mobility by susceptibility-modified solutions as evaluated by cell tracking velocimetry and continuous magnetic sorting. Anal. Chem. 2004;76:3899–3907. [PubMed: 15253623]

26. Jing Y, Moore LR, Williams PS, Chalmers JJ, Farag SS, Bolwell B, Zborowski M. Blood progenitor cell separation from clinical leukapheresis product by magnetic nanoparticle binding and magnetophoresis. Biotechnol. Bioeng. 2007;96:1139–1154. [PubMed: 17009321]

27. Jin X, Yazer MH, Chalmers JJ, Zborowski M. Quantification of changes in oxygen release from red blood cells as a function of age based on magnetic susceptibility measurements. Analyst 2011;136:2996–3003. [PubMed: 21647486]

28. Kim J, Weigand M, Palmer AF, Zborowski M, Yazer MH, Chalmers JJ. Single cell analysis of aged RBCs: quantitative analysis of the aged cells and byproducts. Analyst 2018; DOI: 10.1039/c8an01904e.

29. Zborowski M, Ostera GR, Moore LR, Milliron S, Chalmers JJ, Schechter AN. Red blood cell magnetophoresis. Biophys. J. 2003;84:2638–2645. [PubMed: 12668472]

30. Downey GP, Doherty DE, Schwab B, Elson EL, Henson PM, Worthen GS. Retention of leukocytes in capillaries: role of cell size and deformability. J. Appl. Physiol. 1990;69:1767–78. [PubMed: 2272970]

31. Mollet M, Godoy-Silva R, Berdugo C, Chalmers JJ. Computer simulations of the energy dissipation rate in a fluorescence-activated cell sorter: implications to cells. Biotechnol. Bioeng. 2008;100:260–272. [PubMed: 18078288]

32. Schmid I, Hausner MA, Cole SW, Uittenbogaart CH, Giorgi JV, Jamieson BD. Simultaneous flow cytometric measurement of viability and lymphocyte subset proliferation. J. Immunol. Methods 2001;247:175–186. [PubMed: 11150548]

33. Darabi J, Guo C. Continuous isolation of monocytes using a magnetophoretic-based microfluidic chip. Biomed. Microdevices 2016;18:77. [PubMed: 27518600]

34. Flø RW, Næss A, Lund-Johansen F, Mæhle BO, Sjursen H, Lehmann V, Solberg CO. Negative selection of human monocytes using magnetic particles covered by anti-lymphocyte antibodies. J. Immunol. Methods 1991;137:89–94. [PubMed: 2010620]

Author Manuscript

Author Manuscript

Author Manuscript

Author Manuscript
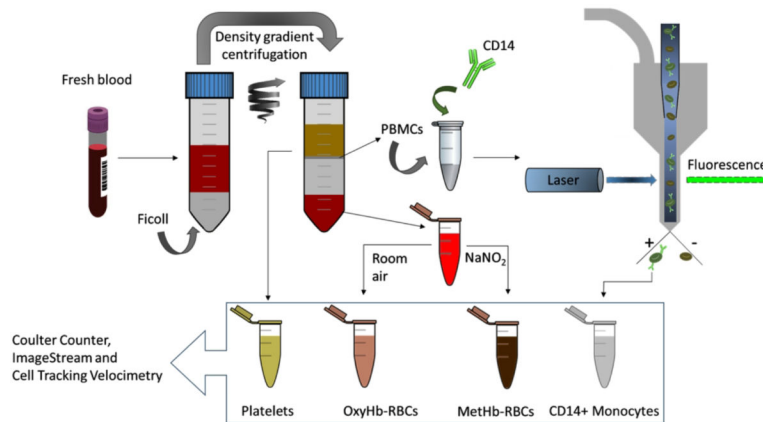
Figure 1.
Workflow of the sample preparation procedure. From each blood sample, four different cell fractions were collected in a consecutive process. Firstly, human fresh whole blood was separated into 3 fractions by density gradient centrifugation: i) platelets, ii) RBCs (oxyhemoglobin RBCs), and iii) PBMCs. The PBMCs were further processed by FACS targeting for CD14+ monocytes. MetHb-RBCs were obtained by treating the OxyHb-RBCs with NaNO2. Afterwards, the four populations were further analyzed using Coulter Counter (size and concentration measurements), ImageStream (for the direct observation of the sorted monocytes) and CTV (magnetic velocity quantification). The same protocol was applied on blood samples from five different donors and the samples were processed within 6 hours of blood draw.
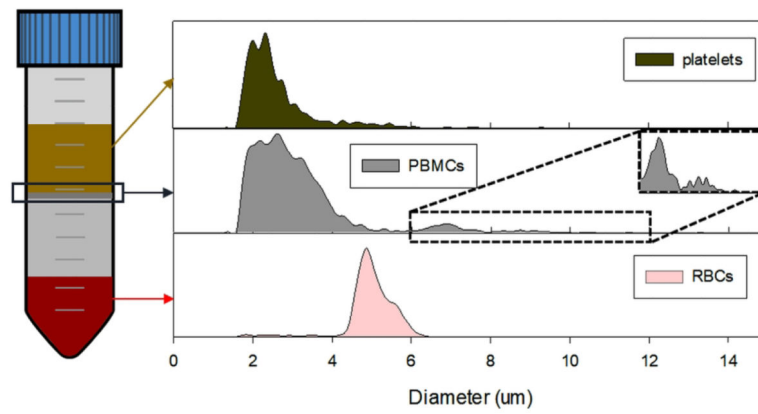
Figure 2.
The histogram of size distribution of the Ficoll-separated entities characterized by Coulter Counter. The PBMCs fraction have three population, the platelet-sized contamination, lymphocytes (6–8 μm) and bigger sized monocyte subpopulation.
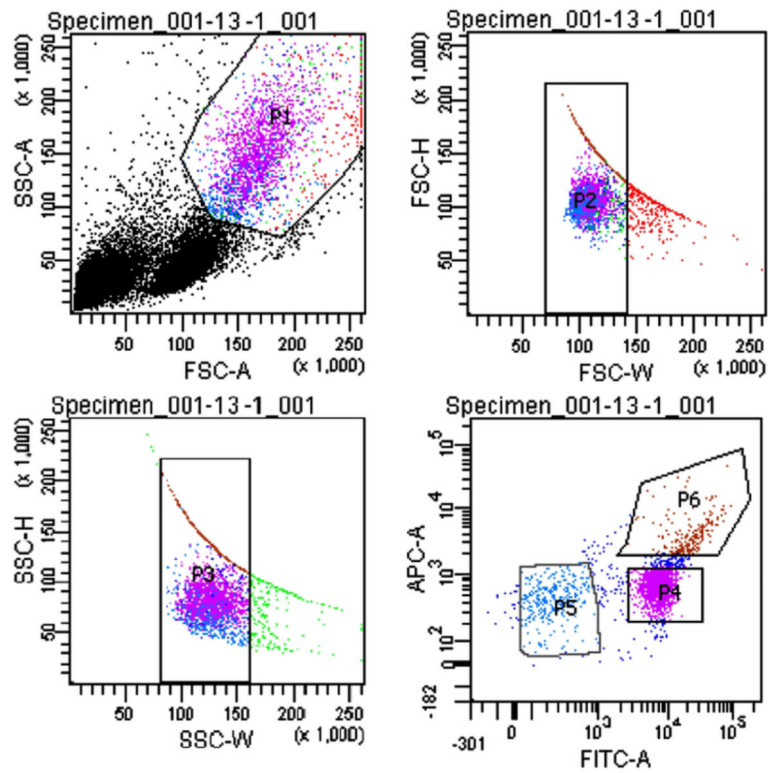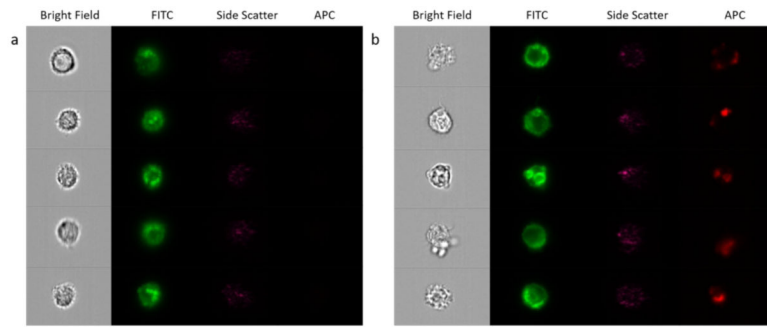
Figure 3.
Flow sorting results for monocyte isolation. P4 represents the CD14+ population, P6 is the CD14+CD61+ fraction and P5 is the CD14-CD61-fraction.
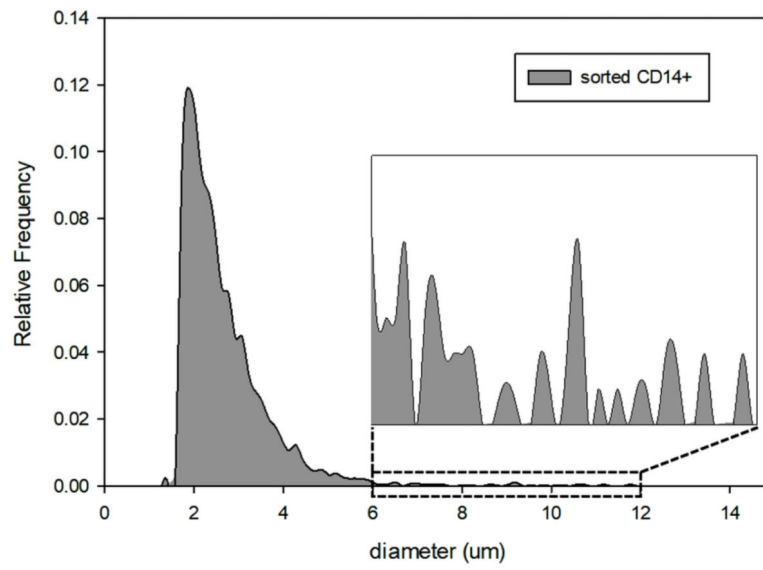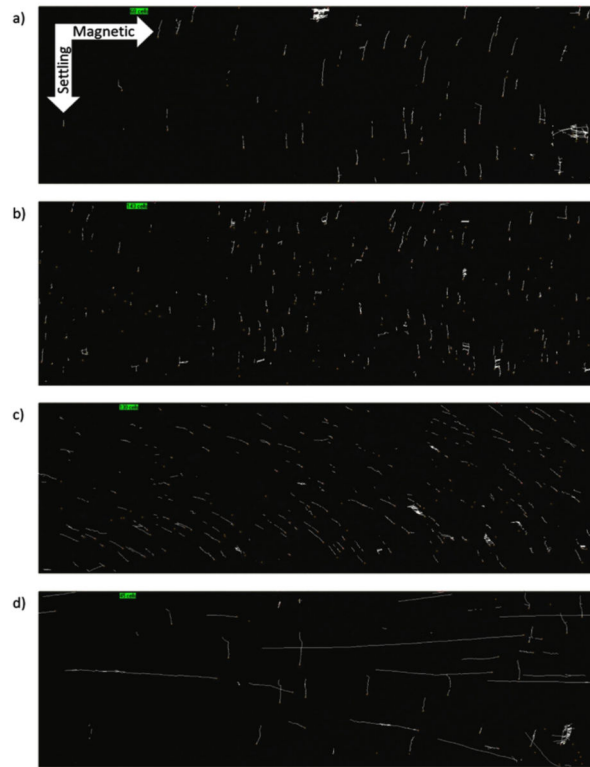
Figure 4.
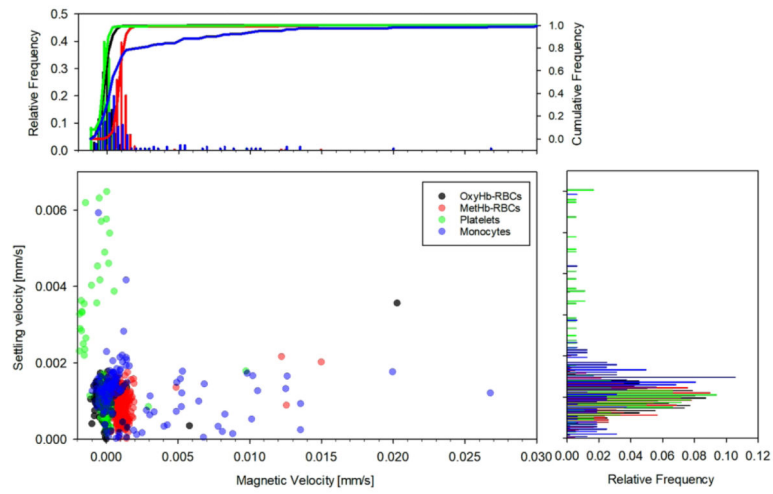Coulter Counter size analysis for the sorted CD14+ sample.

Figure 5.
Images taken from the CD14+ fraction after sorting on ImageStream, showing bright field images, FITC fluorescence intensity and side scatter.
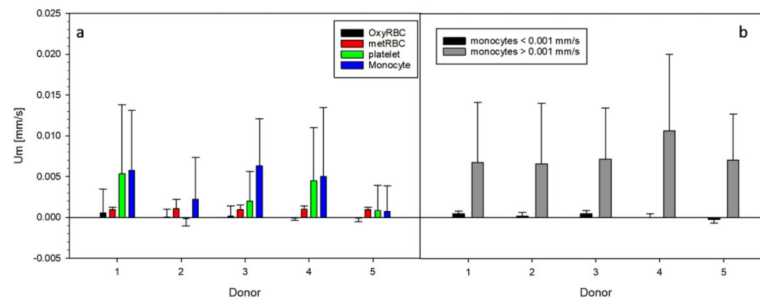
Figure 6.
Trajectories followed by blood cells within the CTV instrument in 50 seconds. a) Platelets; b) OxyHb-RBCs; c) MetHb-RBCs; d) Monocytes.

Figure 7.
Comparison between the magnetic and settling velocities for the four cell fractions obtained from one of the donors.

Figure 8.
Figure 8a: Magnetic velocities reported by the four cell fractions isolated from the five donors blood. Figure 8b: Magnetic velocities of the two monocytes sub-group, higher/lower than 0.001 mm/s.

Table 1.

Size distribution of Ficoll-separated entities from whole blood.

Entity	Size distribution		
RBCs	4.99 ± 0.63 μm		
PBMCs	2.56 ± 0.69 μm	6.87 ± 0.45 μm	8.95 ± 0.71 μm
Platelets	2.69 ± 1.07 μm		

Table 2.

The magnetic velocity of each fraction (Average ± Standard Deviation)

Donor #	oxyRBCs [mm/s]	metRBCs [mm/s]	Platelets [mm/s]	Monocytes [mm/s]
#1 (Female)	5.51.E-04 ± 2.95.E-03	9.52.E-04 ± 2.81.E-04	5.33.E-03 ± 8.51.E-03	5.74.E-03 ± 7.41.E-03
#2 (Male)	4.34.E-05 ± 9.44.E-04	1.10.E-03 ± 1.10.E-03	−1.41.E-04 ± 9.01.E-04	2.21.E-03 ± 5.14.E-03
#3 (Male)	1.40.E-04 ± 1.28.E-03	9.48.E-04 ± 5.66.E-04	1.99.E-03 ± 3.63.E-03	6.32.E-03 ± 5.80.E-03
#4 (Female)	−6.12.E-05 ± 2.70.E-04	9.85.E-04 ± 4.32.E-04	4.51.E-03 ± 6.53.E-03	4.99.E-03 ± 8.51.E-03
#5 (Male)	−8.58.E-05 ± 4.69.E-04	9.71.E-04 ± 2.94.E-04	8.60.E-04 ± 3.09.E-03	7.14.E-04 ± 3.14.E-03

Table 3:

The magnetic velocity [mm/s] of two sub-population among monocytes from each donors (Average ± Standard Deviation)

Donor #	Monocytes < 0.001 mm/s	Monocytes > 0.001 mm/s
#1	4.67.E-04 ± 3.56.E-04	6.79.E-03 ± 7.38.E-03
#2	1.71.E-04 ± 4.58.E-04	6.62.E-03 ± 7.39.E-03
#3	4.66.E-04 ± 4.02.E-04	7.20.E-03 ± 6.28.E-03
#4	2.45.E-05 ± 4.57.E-04	1.07.E-02 ± 9.38.E-03
#5	−1.99.E-04 ± 4.76.E-04	7.08.E-03 ± 5.64.E-03